Science of the Total Environment 673 (2019) 266–271

Contents lists available at ScienceDirect

Science of the Total Environment

journal homepage: www.elsevier.com/locate/scitotenv

Atomic-scale insights into zeolite-based catalysis in N_2O decomposition

Guangzhi He [a,1], Bo Zhang [a,1], Hong He [a,b,c,*], Xueyan Chen [a,c], Yulong Shan [a,c]

[a] State Key Joint Laboratory of Environment Simulation and Pollution Control, Research Center for Eco-Environmental Sciences, Chinese Academy of Sciences, Beijing 100085, China
[b] Center for Excellence in Regional Atmospheric Environment, Institute of Urban Environment, Chinese Academy of Sciences, Xiamen 361021, China
[c] University of Chinese Academy of Sciences, Beijing 100049, China

HIGHLIGHTS

- The nature of activity of zeolite catalysts in N_2O decomposition was clarified.
- The activity of the ion-exchanged zeolites follows the order Fe ≈ Co > Ni > Cu.
- The catalytic activity of the zeolites is governed by the softness of active sites.
- The higher the softness and the 4s component in the HOMO, the higher the activity.

GRAPHICAL ABSTRACT

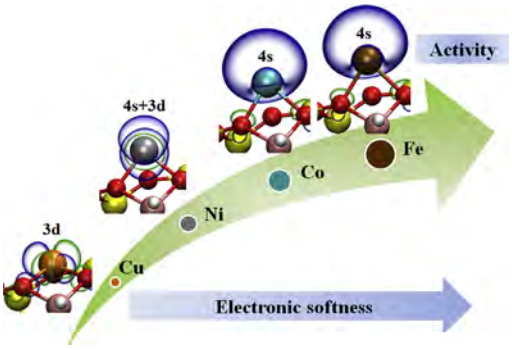

ARTICLE INFO

Article history:
Received 31 January 2019
Received in revised form 29 March 2019
Accepted 31 March 2019
Available online 01 April 2019

Editor: Jianmin Chen

Keywords:
Zeolite
N_2O elimination
Catalytic mechanism
Activity difference
Electronic structure
Density functional theory calculation

ABSTRACT

Nitrous oxide (N_2O) has been the most serious ozone-depleting species throughout the 21st century. Zeolite-based catalysis is a highly promising method for N_2O removal in large-scale industrial applications. However, the exchanged transition metal species in zeolites greatly influence the performance of catalysts. The primary factor governing the catalytic activity is a fiercely debated topic and remains highly uncertain. Here we synthesize a series of transition-metal ion (Fe, Co, Ni, Cu)-exchanged ZSM-5 zeolite catalysts. Both experiments and density functional theory (DFT) calculations demonstrate that the activity for N_2O decomposition follows the order Fe ≈ Co > Ni > Cu. Analysis of the electronic structure properties reveals that the catalytic activity of the transition-metal ion-exchanged ZSM-5 zeolites is governed by the local softness of active sites and the composition of their HOMOs. The higher the local softness and the proportion of 4s orbitals in the HOMO, the higher the catalytic activity, which facilitates electron transfer in the redox process and thereby reduces the reaction barriers for N_2O decomposition into N_2 and O_2. Clarification of the nature of catalytic activity advances the understanding of the principles of zeolite-based catalysis, and is helpful for the design of highly efficient zeolite catalysts for pollutant removals.

1. Introduction

Ozone layer depletion and climate warming are two global environmental problems for the 21st century. Today, nitrous oxide (N_2O) has been the single most important ozone-depleting species throughout the 21st century (Ravishankara et al., 2009). The current global emission

* Corresponding author at: State Key Joint Laboratory of Environment Simulation and Pollution Control, Research Center for Eco-Environmental Sciences, Chinese Academy of Sciences, Beijing 100085, China.
E-mail address: honghe@rcees.ac.cn (H. He).
[1] These authors contributed equally to this work.

https://doi.org/10.1016/j.scitotenv.2019.03.481
0048-9697/

of N_2O arising from anthropogenic activities, such as manufacturing, agriculture, the combustion of fossil fuels, and the application as oxidizers in rocket fuels, is about 1.05×10^7 t/a, which exceeds that of any other ozone-destroying substances, and most likely this will be the case for the rest of the 21st century (Dameris, 2010). N_2O is also a potent greenhouse gas, which has a warming potential 300 times higher than that of CO_2 (Tolman, 2010), and is thus controlled under the Kyoto Protocol. Therefore, development of efficient techniques to reduce N_2O levels in the atmosphere is highly desired to protect the stratospheric ozone layer and diminish the anthropogenic greenhouse effect.

Among various N_2O removal approaches, direct catalytic decomposition using transition-metal ion-exchanged zeolites has been widely accepted as the most promising method for large-scale industrial application due to its high activity, thermal stability, and low cost (Zhang et al., 2016; Melian-Cabrera et al., 2017; Sadovska et al., 2017; Wang et al., 2018). Although some noble metal (e.g., Ru, Rh)-zeolite catalysts exhibit a higher activity for N_2O decomposition in comparison to the low-cost transition-metal zeolites (Kapteijn et al., 1996; Pieterse et al., 2005), the decomposition of N_2O over noble metal catalysts is likely to be poisoned by the presence of NO, O_2 and H_2O (Li and Armor, 1992). This shortcoming, as well as the high cost, restricts large-scale applications of noble metal catalysts for N_2O control. It has been well established that the transition metal species behave as active centers for N_2O decomposition (Pérez-Ramírez et al., 2003; Berlier et al., 2005; Kumar et al., 2006; Guesmi et al., 2010; Rutkowska et al., 2014). Currently, although the reaction pathway of N_2O decomposition is relatively clear (Kondratenko and Pérez-Ramírez, 2006; Liu et al., 2014), the exchanged transition metal species in zeolites greatly influence the performance of the catalysts (Kapteijn et al., 1996; Abu-Zied et al., 2008; Liu et al., 2012), and the intrinsic mechanism remains highly uncertain.

This study aimed to illustrate the chemical principles governing the catalytic activity of the transition-metal ion-exchanged zeolites in N_2O decomposition. For this purpose, a series of transition metal ion (Fe, Co, Ni, Cu)-exchanged ZSM-5 zeolites were prepared, which exhibited dramatic differences in activity for N_2O elimination. The ZSM-5 zeolite was employed as the support because it is widely applied in heterogeneous catalysis, including the elimination of N_2O, due to its excellent catalytic activity and stability (Kapteijn et al., 1996; Sun et al., 2006; Abu-Zied et al., 2008; Zhang et al., 2011). Then, by using density functional theory (DFT) calculations, we revealed the relationship between the electronic structure properties of the exchanged transition metal species and their catalytic performance.

2. Materials and methods

2.1. Catalyst preparation

A series of transition metal ion (Fe, Co, Ni, Cu)-exchanged ZSM-5 zeolites were prepared through the ion-exchange method. H-ZSM-5 ($SiO_2/Al_2O_3 = 25$, Nankai University) was mixed with 0.2 M aqueous solutions of nitrate salts ($Fe(NO_3)_3$, $Co(NO_3)_2$, $Ni(NO_3)_2$, $Cu(NO_3)_2$) at 30 °C for 24 h. The protons located at the Brönsted acid sites were exchanged with transition-metal ions, which formed the active centers. After ion exchange, the samples were filtered, thoroughly washed, then dried at 100 °C overnight. The transition metal ion-exchanged ZSM-5 zeolites were calcined in air at 550 °C for 4 h. The contents of Si, Al, and transition metals within zeolites were determined using inductively coupled plasma-optical emission spectroscopy (ICP-OES, Optima 2000DV). Strong acid solution was used to dissolve the samples before testing. The exchange levels and transition metal contents are shown in Table 1.

2.2. Steady-state experiment

Activity measurements were carried out in a fixed-bed quartz flow reactor (4 mm ID) containing approximately 50 mg of the catalyst (particle size of 125–200 μm). The reactor was heated by a temperature-controlled furnace. A thermocouple was placed on the outside of the reactor tube. A N_2O (1500 ppm)/Ar mixture was introduced into the reactor at GHSV of 35,000 h^{-1}. The reaction products were analyzed by a gas chromatograph (Agilent 6890 N, equipped with a Porapak Q column for the analysis of N_2O and CO_2, and a Molecular Sieve 5A column for the analysis of N_2, O_2 and NO). The reaction system was kept at each reaction temperature for 1 h to reach a steady state before analysis of the product is undertaken. In all measurements, N_2 and O_2 were the only products observed.

Table 1
Turnover frequencies (TOF) for N_2O decomposition at 600 °C and transition metal contents in the ZSM-5 zeolites.

Metal	N_2O conversion (%)	TOF($\times 10^2$) (s^{-1})[a]	Exchange level (%)[b]	Mole of metal ions (10^{-5} mol/g zeolite)
Fe	14.7	1.94	2.0	2.38
Co	15.4	1.41	3.1	3.42
Ni	17.7	0.44	1.49	1.89
Cu	9.6	0.16	24.5	26.8

[a] For calculation of the TOF, 20 mg of Fe- and Co-ZSM-5 and 50 mg of Ni- and Cu-ZSM-5 catalysts were adopted to keep the N_2O conversion below 20%.
[b] The exchange level was estimated on the basis of the metal/Al molar ratio.

2.3. Pulse response experiment

N_2O pulse experiments was performed on a Micromeritics AutoChem II 2920 apparatus, equipped with a computer-controlled CryoCooler and a thermal conductivity detector (TCD). In each experiment, about 50 mg of the catalyst was placed in the U-type quartz reactor. Prior to a pulse-response experiment, the reaction was kept at T_{20} (the temperature of 20% N_2O conversion) for 1 h to reach a steady state. Subsequently, periodic switching of 20% N_2O/Ar to pure Ar was done at intervals of 4 min. Meanwhile, the signals of N_2O ($m/z = 44$), NO ($m/z = 30$), N_2 ($m/z = 28$), and O_2 ($m/z = 32$) were collected simultaneously by mass spectrometry. We adopted a high concentration of N_2O (20%) in the pulse-response experiment to obtain a high-quality mass spectrum of O_2 in the N_2O decomposition reaction.

The turnover frequency (TOF) were calculated with the following equation:

$$TOF = \frac{kp_{N2O}}{n_M} \quad (1)$$

where k is the first-order rate constant (Pirngruber et al., 2007), n_M is the number of active sites (mol/g) obtained by ICP measurements (Table 1), and p_{N2O} is the partial pressure of N_2O. The turnover frequency (TOF) was obtained by keeping N_2O conversion below 20% at 600 °C. Accordingly, 20 mg of Fe- and Co-ZSM-5 and 50 mg of Ni- and Cu-ZSM-5 catalysts were used.

2.4. Computational details

Geometry optimizations and transition state searches were performed at the B3LYP-D3 (Stephens et al., 1994; Grimme et al., 2010)/6-31G(d) (Harihara and Pople, 1973; Francl et al., 1982; Rassolov et al., 1998) level. Vibrational frequencies were calculated at the same level to identify the minima and transition states and to obtain the zero-point vibrational energies. To confirm the transition states and their connected minima, intrinsic reaction coordinate (IRC) calculations (Fukui, 1981) were carried out to trace the reaction pathways. To improve the accuracy of electronic energies, single-point energies at the converged geometries were calculated using the 6-311G(d,p) basis set (Krishnan et al., 1980; McLean and Chandler, 1980) for the main-group elements, and the SDD pseudopotential and basis set (Dolg et al., 1987) for the transition metals (i.e., Fe, Co, Ni, Cu). A double 10-

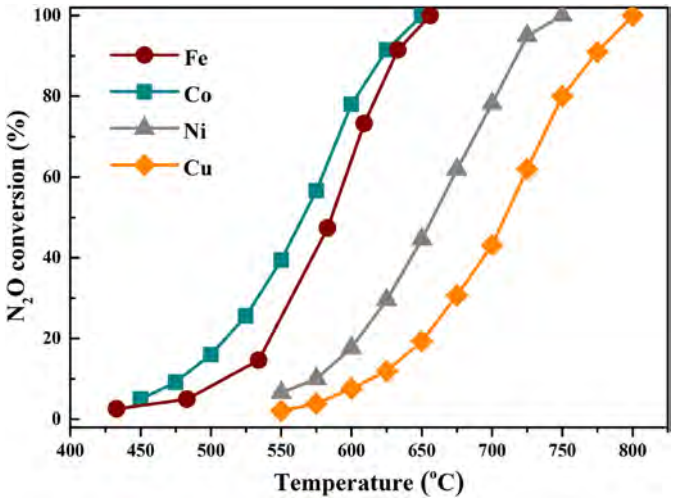

Fig. 1. N_2O conversion over the Fe-, Co-, Ni-, and Cu-ZSM-5 zeolites as a function of temperature in the feed gas of 1500 ppm N_2O/Ar (35,000 h^{-1}).

membered ring ZSM-5 cluster with one Al atom at the T12 site was used as the zeolite model (Olson et al., 1981; Van der Mynsbrugge et al., 2012; Maihom et al., 2013). The 10-membered ring channels (i.e., the main channels of ZSM-5 zeolite) facilitate transport of molecules to the active sites, and thus have been considered to be the main regions where catalytic reactions can take place. The transition metal ion was placed next to the Al-containing tetrahedron. The dangling bonds of boundary Si atoms of all clusters were saturated with H atoms to obtain neutral clusters. All atoms except the H atoms were relaxed. The terminating H atoms were fixed to orient in the Si—O direction in the ZSM-5-type zeolite to avoid unrealistic deformation of the cluster during the geometry optimization (Fellah, 2011). The spin-unrestricted method was applied to the open-shell systems. For a given cluster, all possible spin multiplicities were tested to find the most stable electronic state. All the DFT calculations were performed using the Gaussian 09 package (Frisch et al., 2013). The electronic structure properties of the catalysts were analyzed using a standard wavefunction (WFN) file with the Multiwfn package (Lu and Chen, 2012). The WFN file was produced at the B3LYP-D3/6-31G(d) level using the Gaussian 09 package.

3. Results and discussion

3.1. Catalytic performance

As shown in Table 1, the intrinsic activity, expressed in terms of turnover frequency (TOF), of the different transition metal ion-exchanged ZSM-5 zeolites for the catalytic decomposition of N_2O followed a trend of Fe > Co > Ni > Cu. It is notable that, as the content of Co ions was about 1.5 times as much as that of Fe ions in the zeolite samples (Table 1), the apparent activity of Co-exchanged ZSM-5 was slightly higher than that of Fe-exchanged ZSM-5 (Fig. 1). The Co- and Fe-exchanged ZSM-5 yielded 90% N_2O conversion at about 620 °C, whereas the temperatures for 90% N_2O conversion increased to 710 °C and 760 °C over the Ni- and Cu-exchanged ZSM-5 zeolites, respectively. The exchange level of Cu ions was obviously higher than other transition metal ions (Table 1), which may be due to the fact that Cu ions could be exchanged into the zeolites in various forms (e.g., Cu^{2+}, Cu^{+}, and even CuO) (Deka et al., 2013). Pulse-response experiments (Fig. 2) show that O_2 was generated later than N_2 over these zeolite catalysts, suggesting that the formation and desorption of O_2 from active sites is the rate-determining step for the catalytic cycle.

3.2. DFT calculation

The reaction pathways of N_2O decomposition over a single active site in ZSM-5 zeolites were determined by DFT calculations. The single sites prevail in the zeolite samples (Fig. S1) at low levels of exchange (Table 1) (Zhang et al., 2016). N_2O decomposition over a single active site follows the Eley-Rideal (*E*-R) mechanism and proceeds via three steps [Eq. (2)–(4)]:

$$N_2O + * \rightarrow N_2 + O* \quad (2)$$

$$N_2O + O* \rightarrow N_2 + O_2* \quad (3)$$

$$O_2* \rightarrow O_2 + * \quad (4)$$

where * represents the active sites in zeolite catalysts. Firstly, one N_2O molecule is irreversibly decomposed into N_2 and an adsorbed O atom at the transition-metal active site [Fig. 3a and Eq. (2)]. Subsequently, another N_2O is decomposed into N_2 and adsorbed O at the same site

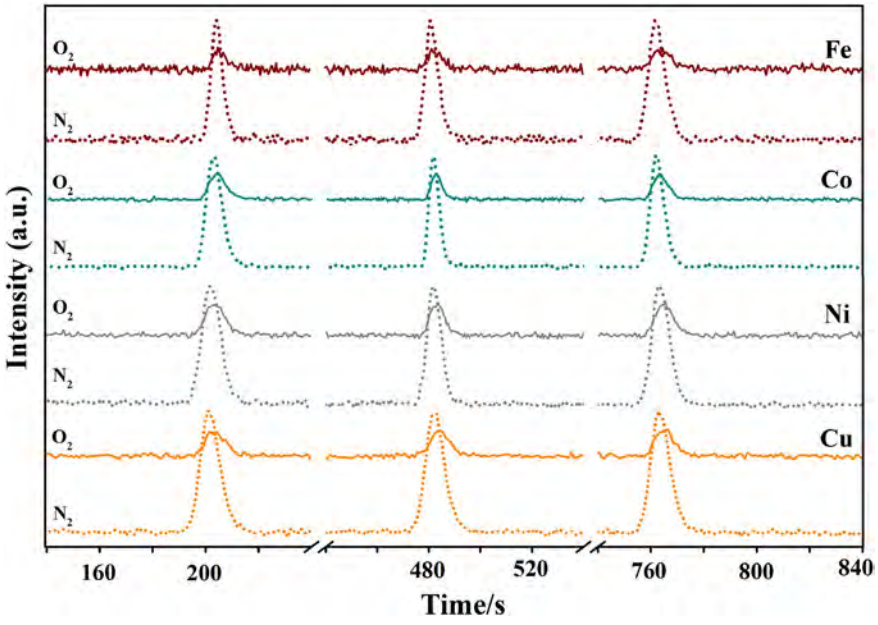

Fig. 2. Pulse-response profiles obtained by periodically switching 20% N_2O/Ar to pure Ar over the transition-metal ion-exchanged ZSM-5 zeolites.

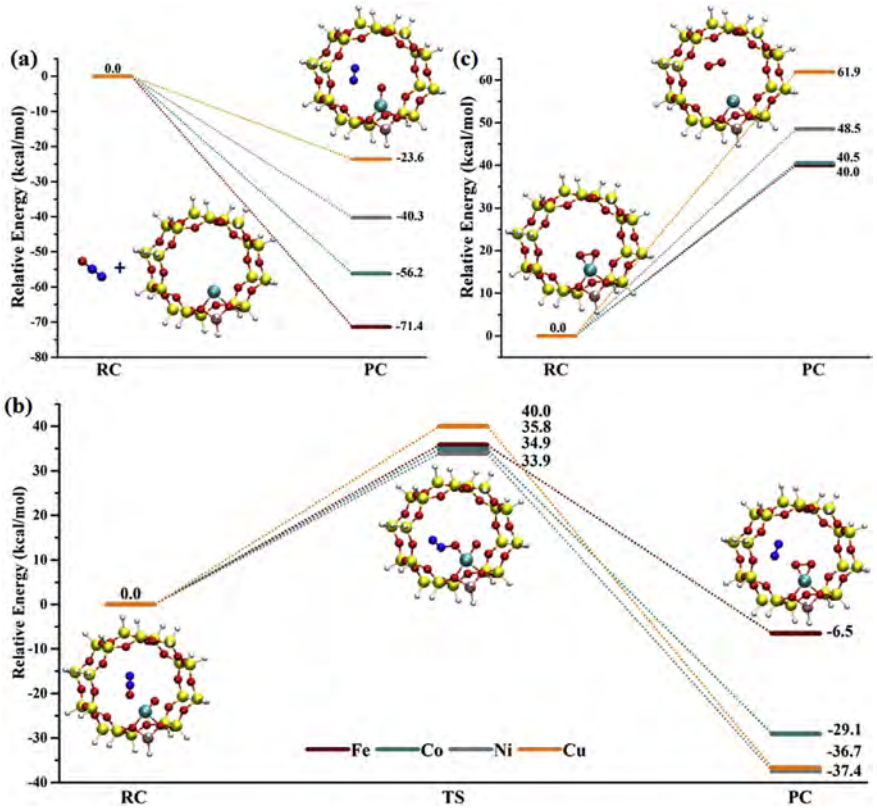

Fig. 3. Zero-point energy-corrected electronic energy profiles of the reaction pathway of N_2O decomposition [(a) and (b)] and O_2 desorption (c) over the transition-metal ion-exchanged ZSM-5 zeolites as well as the optimized geometries of the reactants (RC), transition states (TS), and products (PC) of Co-exchanged ZSM-5. Cyan, red, yellow, pink, and white circles denote Co, O, Si, Al, and H atoms, respectively. The structures of the reactants, transition states, and products for Fe-, Ni- and Cu-exchanged ZSM-5 are shown in Fig. S2–4, respectively. (For interpretation of the references to color in this figure legend, the reader is referred to the web version of this article.)

[Fig. 3b and Eq. (3)]. Finally, the two adsorbed O atoms combine into one O_2 molecule, and then the O_2 desorption regenerates the active site [Fig. 3c and Eq. (4)]. The desorption of O_2 has to overcome an energy barrier significantly higher than the decomposition of N_2O, and thereby is the rate-determining step of the whole catalytic cycle. This DFT-calculated result is consistent with the pulse-response experiment, where the production of O_2 is observably lagging behind that of N_2 (Fig. 2). According to the energy barriers of the rate-determining steps (Fig. 3c), the activity follows the order Fe ≈ Co > Ni > Cu, which agrees well with the experimental activity results (Table 1 and Fig. 1).

To elucidate the nature of the activity differences among the four types of transition metal ions exchanged zeolites, the electronic structure properties of the active sites were analyzed. Local softness is a robust descriptor for reaction activity, which is defined as (Ayers, 2007)

$$S_A^- = Sf_A^- \tag{5}$$

$$S = (VIP - VEA)^{-1} \tag{6}$$

$$f_A^- = q_A(N-1) - q_A(N) \tag{7}$$

where S_A^- is the local softness condensed on the atom A for electrophilic attack, S is the global softness, f_A^- is the electrophilic Fukui function condensed on the atom A, VIP is the vertical ionization potential, VEA is the vertical electron affinity, and $q_A(N)$ and $q_A(N-1)$ are the Hirshfeld charge of atom A for the systems with N and N-1 electrons, respectively. This has been established as a general rule, that is, the higher the local softness, the higher the reactivity of the site. As shown in Table 2, the local softness (S_A^-) follows the same sequence (i.e., Fe > Co > Ni > Cu) as that determined by the energy barriers of the rate-determining steps and the activity experiments. According to the definition above, high local softness implies the electron is easy to transfer in the redox process and thereby lower the catalytic reaction barriers. The orbital composition analysis (Table 2 and Fig. 4) shows that the HOMO is dominated by the Fe and Co 4s orbitals, Ni 4s and 3d orbitals, and Cu 3d orbital in the four types of transition metal ion-exchanged zeolites, respectively. The 4s electrons are generally more active (i.e., softer) than the 3d electrons. Therefore, the high catalytic activity of Fe and Co correlates with the high proportion of 4s orbital in their HOMO, which facilitates electron transfer in the catalytic cycle.

4. Conclusions

This study elucidated the chemical nature of catalytic activity for zeolite-based catalysis in N_2O decomposition for the first time. Direct catalytic decomposition over zeolite-based catalysts could efficiently reduce N_2O levels and mitigate its environmental impacts, including depletion of the ozone layer and the greenhouse effect. In essence, the performance of catalysts is governed by the chemical nature of the transition metal species in zeolites. The relationship between the electronic structure properties of the exchanged transition metal species and their catalytic performance illustrated here advances the understanding of the principles of zeolite-based catalysis and also offers a useful approach

Table 2
Vertical ionization potential (VIP), vertical electron affinity (VEA), electrophilic Fukui function (f_A^-), local softness (S_A^-), and HOMO orbital composition of Fe-, Co-, Ni-, and Cu-ZSM-5 zeolites. Energies are given in Hartrees.

Metal	VIP	VEA	f_A^- [a]	S_A^-	HOMO orbital composition
Fe	0.2406	0.0244	0.61	2.84	4s (56.1%)
Co	0.2419	0.0266	0.58	2.68	4s (55.3%)
Ni	0.2574	0.0166	0.54	2.26	4s (43.7%) + 3d (36.1%)
Cu	0.2741	−0.0220	0.37	1.23	3d (73.3%)

[a] *A* represents Fe, Co, Ni, and Cu, respectively.

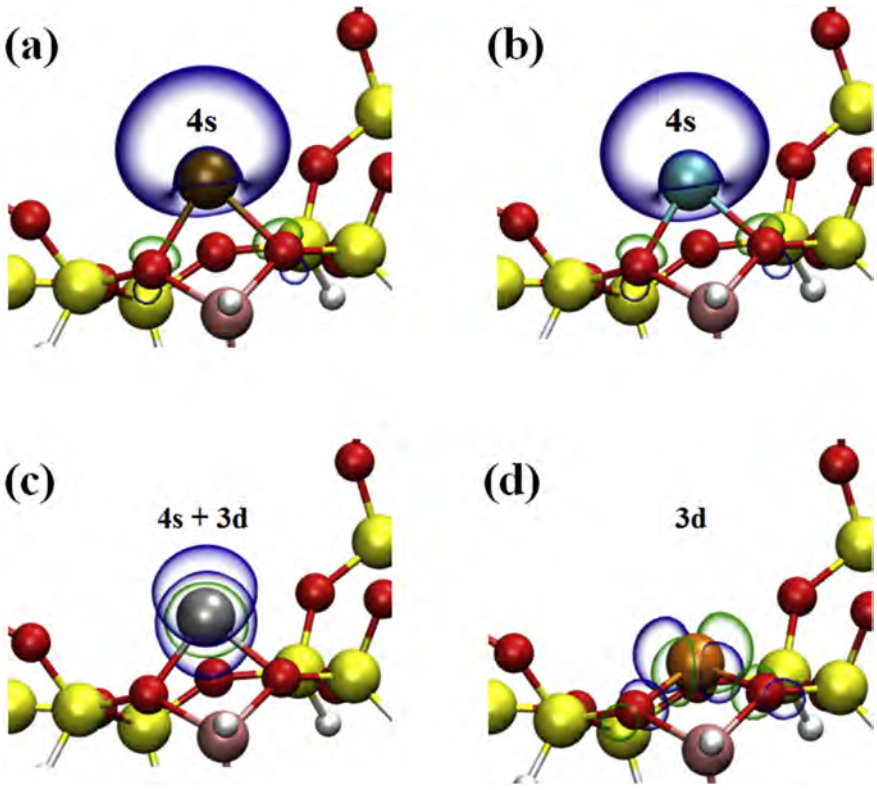

Fig. 4. HOMO orbitals (isovalue = 0.05 a.u.) of Fe (a), Co (b), Ni (c), and Cu (d)-ZSM-5 zeolites. Red, yellow, pink, and white circles denote O, Si, Al, and H atoms, respectively. The large ochre, cyan, gray, and orange circles denote Fe, Co, Ni, and Cu atoms, respectively. (For interpretation of the references to color in this figure legend, the reader is referred to the web version of this article.)

to explore the activity of other catalytic systems (e.g., metal oxide and noble metal catalysts) for pollutant removals.

Conflicts of interest

The authors declare no competing financial interest.

Acknowledgement

This work is supported by the National Natural Science Foundation of China (21637005, 21777171) and the Youth Innovation Promotion Association of Chinese Academy of Sciences (2019045).

Appendix A. Supplementary data

Supplementary data to this article can be found online at https://doi.org/10.1016/j.scitotenv.2019.03.481.

References

Abu-Zied, B.M., Schwieger, W., Unger, A., 2008. Nitrous oxide decomposition over transition metal exchanged ZSM-5 zeolites prepared by the solid-state ion-exchange method. Appl. Catal., B 84, 277–288.
Ayers, P.W., 2007. The physical basis of the hard/soft acid/base principle. Faraday Discuss. 135, 161–190.
Berlier, G., Ricchiardi, G., Bordiga, S., Zecchina, A., 2005. Catalytic activity of Fe ions in iron-based crystalline and amorphous systems: role of dispersion, coordinative unsaturation and Al content. J. Catal. 229, 127–135.
Dameris, M., 2010. Depletion of the ozone layer in the 21st century. Angew. Chem. Int. Ed. 49, 489–491.
Deka, U., Lezcano-Gonzalez, I., Weckhuysen, B.M., Beale, A.M., 2013. Local environment and nature of Cu active sites in zeolite-based catalysts for the selective catalytic reduction of NO_x. ACS Catal. 3, 413–427.
Dolg, M., Wedig, U., Stoll, H., Preuss, H., 1987. Energy adjusted ab initio pseudopotentials for the first row transition elements. J. Chem. Phys. 86, 866–872.
Fellah, M.F., 2011. CO and NO adsorptions on different iron sites of Fe-ZSM-5 clusters: a density functional theory study. J. Phys. Chem. C 115, 1940–1951.
Francl, M.M., Pietro, W.J., Hehre, W.J., Binkley, J.S., Gordon, M.S., Defrees, D.J., Pople, J.A., 1982. Self-consistent molecular orbital methods. XXIII. A polarization-type basis set for second-row elements. J. Chem. Phys. 77, 3654–3665.
Frisch, M.J., Trucks, G.W., Schlegel, H.B., Scuseria, G.E., Robb, M.A., Cheeseman, J.R., Scalmani, G., Barone, V., Mennucci, B., Petersson, G.A., Nakatsuji, H., Caricato, M., Li, X., Hratchian, H.P., Izmaylov, A.F., Bloino, J., Zheng, G., Sonnenberg, J.L., Hada, M., Ehara, M., Toyota, K., Fukuda, R., Hasegawa, J., Ishida, M., Nakajima, T., Honda, Y., Kitao, O., Nakai, H., Vreven, T., Montgomery Jr., J.A., Peralta, J.E., Ogliaro, F., Bearpark, M., Heyd, J.J., Brothers, E., Kudin, K.N., Staroverov, V.N., Kobayashi, R., Normand, J., Raghavachari, K., Rendell, A., Burant, J.C., Iyengar, S.S., Tomasi, J., Cossi, M., Rega, N., Millam, N.J., Klene, M., Knox, J.E., Cross, J.B., Bakken, V., Adamo, C., Jaramillo, J., Gomperts, R., Stratmann, R.E., Yazyev, O., Austin, A.J., Cammi, R., Pomelli, C., Ochterski, J.W., Martin, R.L., Morokuma, K., Zakrzewski, V.G., Voth, G.A., Salvador, P., Dannenberg, J.J., Dapprich, S., Daniels, A.D., Farkas, O., Foresman, J.B., Ortiz, J.V., Cioslowski, J., Fox, D.J., 2013. Gaussian 09, Revision D.01. Gaussian, Inc., Wallingford CT.
Fukui, K., 1981. The path of chemical reactions-the IRC approach. Acc. Chem. Res. 14, 363–368.
Grimme, S., Antony, J., Ehrlich, S., Krieg, H., 2010. A consistent and accurate ab initio parametrization of density functional dispersion correction (DFT-D) for the 94 elements H-Pu. J. Chem. Phys. 132, 154104.
Guesmi, H., Berthomieu, D., Kiwi-Minsker, L., 2010. Reactivity of oxygen species formed upon N_2O dissociation over Fe-ZSM-5 zeolite: CO oxidation as a model. Catal. Commun. 11, 1026–1031.
Harihara, P.C., Pople, J.A., 1973. The influence of polarization functions on molecular orbital hydrogenation energies. Theor. Chim. Acta 28, 213–222.
Kapteijn, F., Rodriguez-Mirasol, J., Moulijn, J.A., 1996. Heterogeneous catalytic decomposition of nitrous oxide. Appl. Catal., B 9, 25–64.
Kondratenko, E.V., Pérez-Ramírez, J., 2006. Mechanism and kinetics of direct N_2O decomposition over Fe-MFI zeolites with different iron speciation from temporal analysis of products. J. Phys. Chem. B 110, 22586–22595.
Krishnan, R., Binkley, J.S., Seeger, R., Pople, J.A., 1980. Self-consistent molecular orbital methods. XX. A basis set for correlated wave functions. J. Chem. Phys. 72, 650–654.
Kumar, M.S., Pérez-Ramírez, J., Debbagh, M.N., Smarsly, B., Bentrup, U., Brückner, A., 2006. Evidence of the vital role of the pore network on various catalytic conversions of N_2O over Fe-silicalite and Fe-SBA-15 with the same iron constitution. Appl. Catal., B 62, 244–254.
Li, Y.J., Armor, J.N., 1992. Catalytic decomposition of nitrous oxide on metal exchanged zeolites. Appl. Catal., B 1, L21–L29.
Liu, N., Zhang, R., Chen, B., Li, Y., Li, Y., 2012. Comparative study on the direct decomposition of nitrous oxide over M (Fe, Co, Cu)-BEA zeolites. J. Catal. 294, 99–112.
Liu, N., Zhang, R., Li, Y., Chen, B., 2014. Local electric field effect of TMI (Fe, Co, Cu)-BEA on N_2O direct dissociation. J. Phys. Chem. C 118, 10944–10956.

Lu, T., Chen, F., 2012. Multiwfn: a multifunctional wavefunction analyzer. J. Comput. Chem. 33, 580–592.
Maihom, T., Wannakao, S., Boekfa, B., Limtrakul, J., 2013. Density functional study of the activity of gold-supported ZSM-5 zeolites for nitrous oxide decomposition. Chem. Phys. Lett. 556, 217–224.
McLean, A.D., Chandler, G.S., 1980. Contracted Gaussian basis sets for molecular calculations. I. Second row atoms, Z=11-18. J. Chem. Phys. 72, 5639–5648.
Melian-Cabrera, I., van Eck, E.R.H., Espinosa, S., Siles-Quesada, S., Falco, L., Kentgens, A.P.M., Kapteijn, F., Moulijn, J.A., 2017. Tail gas catalyzed N_2O decomposition over Fe-beta zeolite. On the promoting role of framework connected AlO_6 sites in the vicinity of Fe by controlled dealumination during exchange. Appl. Catal., B 203, 218–226.
Olson, D.H., Kokotailo, G.T., Lawton, S.L., Meier, W.M., 1981. Crystal structure and structure-related properties of ZSM-5. J. Phys. Chem. 85, 2238–2243.
Pérez-Ramírez, J., Kapteijn, F., Bruckner, A., 2003. Active site structure sensitivity in N_2O conversion over FeMFI zeolites. J. Catal. 218, 234–238.
Pieterse, J.A.Z., Mul, G., Melian-Cabrera, I., van den Brink, R.W., 2005. Synergy between metals in bimetallic zeolite supported catalyst for NO-promoted N_2O decomposition. Catal. Lett. 99, 41–44.
Pirngruber, G.D., Roy, P.K., Prins, R., 2007. The role of autoreduction and of oxygen mobility in N_2O decomposition over Fe-ZSM-5. J. Catal. 246, 147–157.
Rassolov, V.A., Pople, J.A., Ratner, M.A., Windus, T.L., 1998. 6-31G* basis set for atoms K through Zn. J. Chem. Phys. 109, 1223–1229.
Ravishankara, A.R., Daniel, J.S., Portmann, R.W., 2009. Nitrous oxide (N_2O): the dominant ozone-depleting substance emitted in the 21st century. Science 326, 123–125.
Rutkowska, M., Chmielarz, L., Macina, D., Piwowarska, Z., Dudek, B., Adamski, A., Witkowski, S., Sojka, Z., Obalová, L., Van Oers, C.J., Cool, P., 2014. Catalytic decomposition and reduction of N_2O over micro-mesoporous materials containing Beta zeolite nanoparticles. Appl. Catal., B 146, 112–122.
Sadovska, G., Tabor, E., Sazama, P., Lhotka, M., Bernauer, M., Sobalik, Z., 2017. High temperature performance and stability of Fe-FER catalyst for N_2O decomposition. Catal. Commun. 89, 133–137.
Stephens, P.J., Devlin, F.J., Chabalowski, C.F., Frisch, M.J., 1994. Ab initio calculation of vibrational absorption and circular dichroism spectra using density functional force fields. J. Phys. Chem. 98, 11623–11627.
Sun, K., Xia, H., Hensen, E., van Santen, R., Li, C., 2006. Chemistry of N_2O decomposition on active sites with different nature: effect of high-temperature treatment of Fe/ZSM-5. J. Catal. 238, 186–195.
Tolman, W.B., 2010. Binding and activation of N_2O at transition-metal centers: recent mechanistic insights. Angew. Chem. Int. Ed. 49, 1018–1024.
Van der Mynsbrugge, J., Hemelsoet, K., Vandichel, M., Waroquier, M., Van Speybroeck, V., 2012. Efficient approach for the computational study of alcohol and nitrile adsorption in H-ZSM-5. J. Phys. Chem. C 116, 5499–5508.
Wang, A., Wang, Y., Walter, E.D., Kukkadapu, R.K., Guo, Y., Lu, G., Weber, R.S., Wang, Y., Peden, C.H.F., Gao, F., 2018. Catalytic N_2O decomposition and reduction by NH_3 over Fe/Beta and Fe/SSZ-13 catalysts. J. Catal. 358, 199–210.
Zhang, B., Lu, Y., He, H., Wang, J., Zhang, C., Yu, Y., Xue, L., 2011. Experimental and density functional theory study of the adsorption of N_2O on ion-exchanged ZSM-5: part II. The adsorption of N_2O on main-group ion-exchanged ZSM-5. J. Environ. Sci. 23, 681–686.
Zhang, R., Liu, N., Lei, Z., Chen, B., 2016. Selective transformation of various nitrogen-containing exhaust gases toward N_2 over zeolite catalysts. Chem. Rev. 116, 3658–3721.